Computational Analysis of Flows of a Lobed Mixer Nozzle using LES

Yoshinori OOBA, Hidekazu KODAMA, Yoshiya NAKAMURA
Ishikawajima-Harima Heavy Industries Co., Ltd.
229 Tonogaya, Mizuho-machi, Nishitama-gun, Tokyo, 190-1297, JAPAN
yoshinori_ooba@ihi.co.jp

Osamu NOZAKI, Kazuomi YAMAMOTO, Toshio NISHIZAWA
Japan Aero-Space Exploration Agency
7-44-1 Jindaijihigashi, Chofu, Tokyo, 182-8522, JAPAN

Keywords: Lobed Mixer Nozzle, LES, Jet Noise

Abstract

ESPR project started in 1999 with METI and NEDO support as five-years program in order to develop necessary technologies for the next-generation SST engine. In ESPR program, jet noise reduction technologies are focused as environmentally compatible technologies, which are critical to realize next-generation SST. In designing a lobed mixer nozzle which is a jet noise suppression system, there are many difficulties to understand the detailed flow phenomena occurred in the system because of its complexity. Large Eddy Simulation (LES) was applied to the lobed mixer nozzle flow analysis in ESPR project. The results demonstrated that LES approach was capable of predicting mixing characteristics of a complicated flow.

Introduction

A very important requirement to be satisfied in developing the next-generation supersonic transport (SST) is to introduce techniques for noise reductions at taking off and landing. It is known that the major source of the noise at these flight modes is a jet flow exhausted from an air-breathing engine. The jet noise is generated by the turbulent mixing of the jet flow with the external air stream. A lobed mixer nozzle which consists of a splitter plate with convoluted trailing edge is the forced mixing device that reduces the high-speed velocity regions of the jet. Technology for satisfied jet noise reduction using the lobed mixer nozzle requires to understand the detailed mixing mechanism. However there are many difficulties to understand the detailed flow phenomena occurred in the noise suppression system because of its complexity.

Reynolds Averaged Navier-Stokes (RANS) approach is commonly used to predict turbulent flows for many applications. CFD simulations using the RANS approach were conducted for the lobed mixer nozzle system conducted by Nakamura et al.[1] with two kinds of turbulence models, the Baldwin-Lomax (B-L model)[2] and Lam-Bremhorst k- ε turbulence model (L-B model)[3]. The solutions were compared with the measured data of the high Reynolds number aerodynamic tests for the lobed mixer nozzle system. In the experimental tests, three high velocity core regions clearly appeared at the center of the ejector duct and both upper and lower lobe ends, whereas the RANS simulations showed quite different velocity profiles at the outlet of the ejector duct. This indicates that the RANS approach using simplistic turbulence models like the B-L model or the L-B model is not adequate for proper prediction of the complicated mixing phenomena.

Recently, with increasing computer power, it has become possible to investigate the detailed flow structures of a jet flow through a three dimensional Direct Numerical Simulation (DNS). Freund et al. performed DNS to predict a supersonic round jet and presented the detailed mixing mechanism of the jet flow[4]. However, DNS requires sufficient computer capacity to resolve all of the time and length scales associated with high Reynolds number flows. In the practical applications, such simulations are clearly beyond the capacity of today's most advanced computers.

Large Eddy Simulation (LES) in which the large scales of the turbulence are resolved on the computational grid and the small scales are modeled is a compromise between DNS and RANS approach. The advantage of the LES method is that it is possible to calculate flows with high Reynolds numbers at a reasonable computational cost. Choi et al.[5] conducted LES to predict the high-Reynolds number jet flow of a convergent-divergent axisymmetric nozzle (CD nozzle) which was tested by Yamamoto et at.[6]. It was demonstrated that three dimensional LES accurately predicted the characteristics of the turbulence for the round jet flowfield.

In ESPR project, which started in 1999 with METI and NEDO support in order to develop necessary technologies for the next-generation SST engine, jet noise reduction technologies were focused as environmentally compatible technologies and LES was applied to the flowfield downstream of a lobed mixer nozzle in order to understand its detailed mixing mechanism[7-8]. The present paper introduces the LES applications conducted in ESPR project and demonstrates the capability of LES to predict the mixing characteristics of complicated flows.

Numerical procedure

The governing equations were the Favre-filtered three dimensional compressible Navier-Stokes equations. The convection terms were discretized using the fourth order upwind scheme. Smagorinsky SGS model with Smagorinsky constant 0.15 was introduced to determine the subgrid turbulence viscosity[9]. In near-wall regions, Smagorinsky constant was multiplied by the van Driest damping factor for the eddy viscosity to attain a more correct limiting behavior. For unsteady flow calculations, an implicit method with a Newton sub-iteration method was applied to obtain a converged solution at every time step.

In the present calculation, multiblock method with parallel computation algorithm was introduced to use large computational domain with necessary grid refinement. The calculation of each sub-domain was executed on a different processing element of Numerical Wind Tunnel (NWT), which was a parallel supercomputer developed by Japan Aero-Space Exploration Agency (JAXA) (see Fig. 1). Each sub-domain exchanged boundary information with neighboring sub-domains.

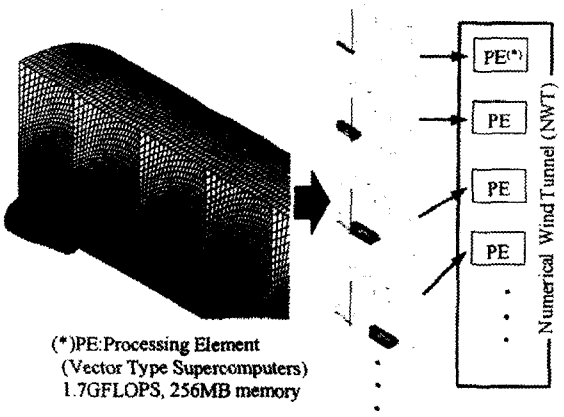

Fig. 1 Schematic of parallel computing (CD nozzle model)

Boundary conditions

At the inflow boundary, the radial distributions of total temperature, total pressure and flow angle were imposed. Non-slip and adiabatic wall boundary conditions were applied to mixer nozzle surfaces. At the far field boundary, total pressure and flow angle were imposed and the magnitude of velocity was extrapolated in the radial direction.

Results and discussion

CD NOZZLE MODEL

A RANS analysis using L-B mode and a LES analysis were first conducted in order to clarify the differences of capability to predict the flowfield downstream of the CD nozzle exit between these simulations (see Fig.2). Table 1 shows the design parameters for the CD nozzle which was tested by Yamamoto et al[6]. In the calculation, 1/4 annular block was simulated using circumferential periodic boundary conditions at circumferential boundary ends. Structured grids were arranged to fit the surfaces of the CD nozzle.

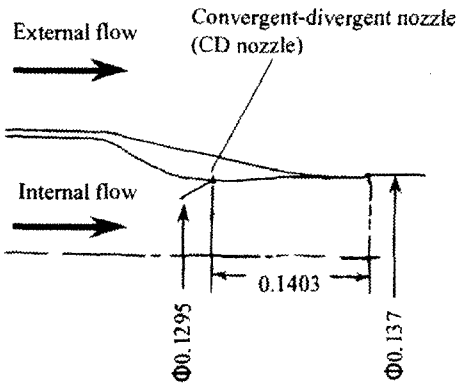

Fig. 2 Schematic of CD nozzle

Table 1 Test condition of CD nozzle

Exit velocity (m/s)	734.3
Ambient velocity (m/s)	121.9
Pressure ratio	3.121
Stagnation temperature (K)	953.3

The computational domain extended 15.0Deq in the streamwise direction and 4.0Deq in the radial direction. Here, Deq is the equivalent diameter of the jet flow and Deq became 0.129m in the test. The domain was divided into thirteen sub-domains and a structured grid was used for each sub-domain. The total number of the computational mesh was about 2.6 million for both of L-B model and LES. At inflow boundary in the mixer nozzle, a random fluctuation was neglected.

Figure 3 shows the instantaneous Mach number contours both of the LES analysis and RANS analysis using L-B model. The red region represents the high velocity region.

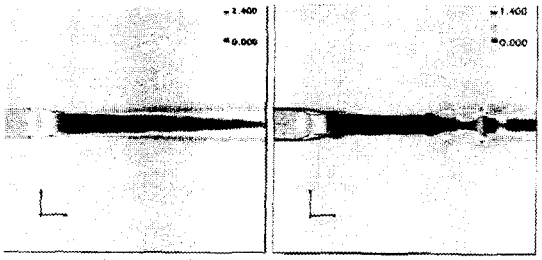

(a) L-B model (b) LES

Fig. 3 Instantaneous Mach number distribution of CD nozzle

The L-B mode result predicted that the high velocity region mixed with the ambient flow downstream of the nozzle exit and that the long extend potential core region existed along the centerline (see Fig. 3 (a)). In the L-B result, it can be seen that the mixing layer between the potential core and the mean flow constantly grew in the axial direction. On the other hand, LES predicted the detailed vortex structure in the mixing layer (see Fig. 3 (b)).

In figure 4, temporally averaged axial velocity profiles of the LES results are compared with the measured data at two axial locations downstream of the CD nozzle, X=0.2Deq and X=4.4Deq. The measured data was acquired by traversing probes in the axial directions. U was the axial velocity component. R and X were the radial and axial position, respectively. These parameters were normalized using Uj and Deq. Here, Uj is the axial velocity component at the outlet of CD nozzle. The agreement between the measurement data and the LES result is quite good at both axial locations. The results of L-B model predicted a similar distribution as the results of LES at 0.4Deq axial location (see Fig. 4 (a)). However, the radially thicker profile of the mixing layer was predicted at 4.4Deq axial location (see Fig. 4 (b)). This indicates that L-B model predicted faster mixing in the flowfield than LES. From these results, it seems that the LES has capability of predicting more realistic mixing phenomena occurred in the mixing layer by simulating the more detailed turbulent structures.

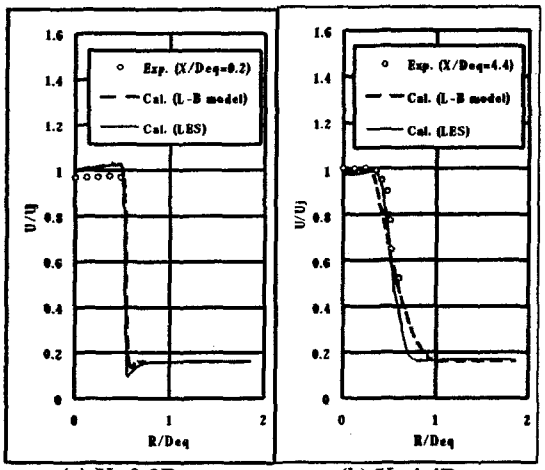

(a) X=0.2Deq (b) X=4.4Deq

Fig. 4 Comparisons of axial velocity components behind outlet of CD nozzle

LOBED MIXER NOZZLE MODEL

Experiment

Particle Image Velocimetry (PIV) was used in order to understand the complicated flowfield downstream of the lobed mixer nozzle exit. The benefit of PIV is that it provides the simultaneous visualization of the two-dimensional streamline pattern in unsteady flows as well as the quantification of the velocity field over the plane.

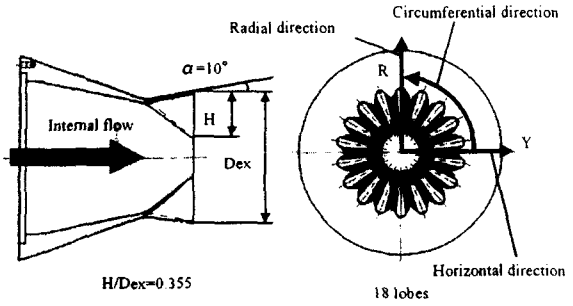

(a) Cross section (b) Outlet shape of lobed mixer nozzle

Fig. 5 Schematic of 18-lobe convoluted mixer nozzle

Figure 5 shows the schematic of the 18-lobe convoluted mixer nozzle used in the experiment. In the figure, H and Dex denote the lobe height and the diameter of the nozzle at the exit, respectively. The penetration ratio H/Dex is 0.355 and the forced angle α is 10 degrees at the exit of the lobed mixer nozzle.

The experimental studies were conducted in the anechoic wind tunnel of IHI. Figure 6 shows a schematic of the PIV measurement system. The PIV system consists of a Nd-Yag laser, light sheet beam forming optics and a single CCD camera which had a resolution of 1280×1024 pixels. Particles (1.0 μ m diameter SiO_2) were introduced as seeds for PIV measurement into the upstream of the mixer nozzle. Traverse for laser measurement was capable in the horizontal direction. Data was acquired at a streamwise plane of the flow corresponding to the symmetry axis of the lobed mixer nozzle (A-A plane in Fig. 7) and one plane parallel to the A-A plane at horizontal locations and Y=0.292Dex (B-B plane in Fig. 7). At each plane 200 images were acquired and the data was ensemble-averaged to produce mean flow.

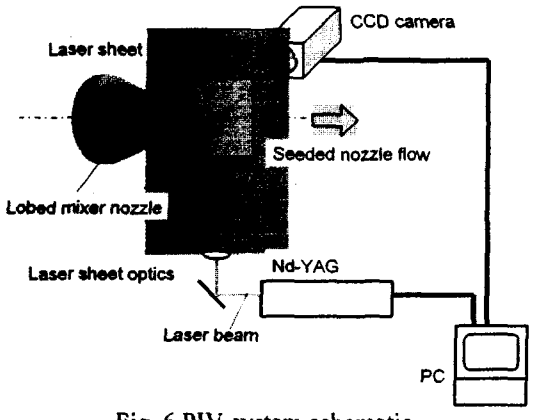

Fig. 6 PIV system schematic

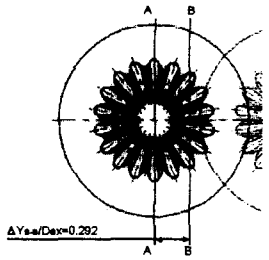

Fig. 7 Measurement planes of PIV

In the test, nozzle pressure ratio (NPR) was 1.19 and the total temperature ratio was 1.01. A Reynolds number based on Dex and the mean velocity magnitude (Uex) was about 1,000,000. Here NPR was defined with respect to the ambient pressure and Uex was calculated by NPR and the total temperature.

Computational results

In the calculation, only one lobe domain was simulated using circumferential periodic boundary conditions at circumferential boundary ends (see Fig. 8 (a)). The computational domain extended 12.5Dex in the streamwise direction and 4.9Dex in the radial direction (see Fig. 8 (b)).

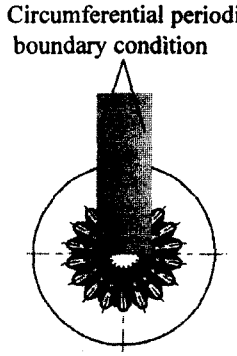

(a) Circumferential periodic boundary condition

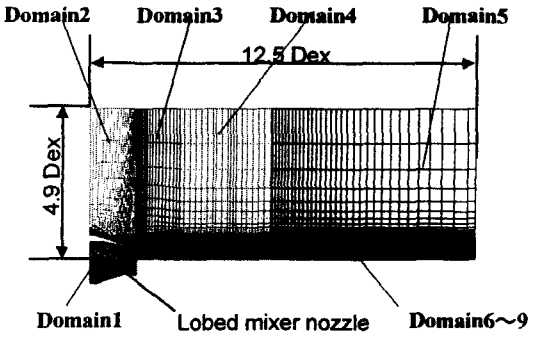

(b) Domain decomposition

Fig. 8 Computational domain

The domain was divided into nine sub-domains and a structured grid was used for each sub-domain. The total number of the computational mesh was about 7.5 million. At inflow boundary in the mixer nozzle, a random fluctuation was added to the velocity components and the resultant turbulence intensity at the centerline near the mixer nozzle exit was 5% of Uex. From the measurement, it was found that the turbulence intensity was about 10% of Uex there. The calculation with larger amplitude of fluctuation became unstable, so that the same level of turbulence intensity as the experiment could not be achieved in the calculation.

Figure 9 (a) shows the instantaneous distribution of the simulated velocity magnitude of the flowfield downstream of the lobed mixer nozzle. In the figure, the transparent iso-surface indicates the low velocity region and the region inside the low velocity region represents the high velocity core region downstream of the mixer nozzle. It can be seen that the high velocity region from the mixer nozzle exit rapidly mixed with the ambient air. Figure 9 (b) shows the distribution of the instantaneous vorticity strength around the axis of the lobed mixer nozzle. The LES results predicted the inherent three-dimensional structure of turbulence downstream of the mixer nozzle.

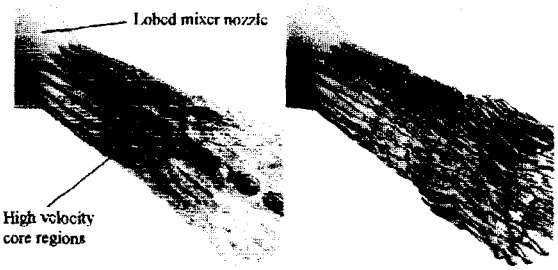

(a) Velocity magnitude (b) Vorticity strength around axis ($\omega x = \pm 10$)

Fig. 9 Iso-surfaces of instantaneous flowfield downstream of lobed mixer nozzle

Figures 10 (a) and 10 (b) show the time-averaged contours of measured velocity magnitude at planes A-A and B-B, respectively. The red color represents a high velocity region. The measured data shows appreciable mixing including high velocity core regions occurred downstream of the mixer nozzle exit. It can be seen that two kinds of core region exist, 1) the long-extended core region along the centerline and 2) the finite core regions from upper and lower lobes in Fig. 10 (a). The long-extended core region shows that only little mixing occurs around this region. On the contrary, it is seen in Fig. 10 (b) that low-velocity regions start from the inner ends of the lobes expanding rapidly to the downstream. This shows that a fair degree of mixing occurs as a result of viscous shear between two streams produced by the lobes.

(a) PIV (A-A plane) (c) LES (A-A plane)

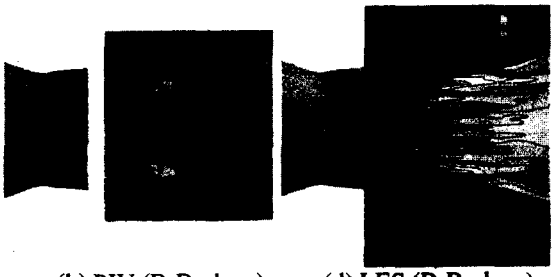

(b) PIV (B-B plane) (d) LES (B-B plane)

Fig. 10 Time-averaged velocity contours of PIV data at different measurement locations

Figures 10 (c) and 10 (d) show the time-averaged contours of calculated velocity magnitude at planes A-A and B-B, respectively. For the purpose of comparison between measurement and calculation, the magnitudes of calculated velocity component projected on the measurement planes are presented in Fig. 10 (a) and 10 (b), because the current PIV system was only capable of measuring flow field vectors in two dimensions. It can be seen that the LES results capture the above-mentioned overall features of the measured flow structure downstream of the lobed mixer nozzle.

Comparison of radial profiles of the axial velocities between measurement and calculation at 1.0Dex and 1.5Dex downstream from the mixer nozzle exit on the A-A plane (see Fig. 11) are shown in Fig. 12 (a) and 12 (b), respectively. The axial velocity component U was normalized by Uex and the radial distance R was normalized by Dex. A good agreement was obtained between the measured and calculated radial profile at 1.0Dex (see Fig. 12 (a)). At 1.5Dex, the levels of the three velocity peaks for the respective core regions reasonably agree between measurement and calculation, however there are small discrepancy between the two results concerning the radial locations of the velocity peaks which appear downstream of the upper and lower lobes (see Fig. 12 (b)).

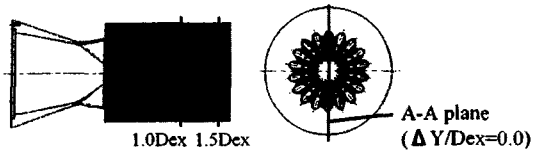

Fig.11 Axial locations of comparison between the PIV data and the LES results

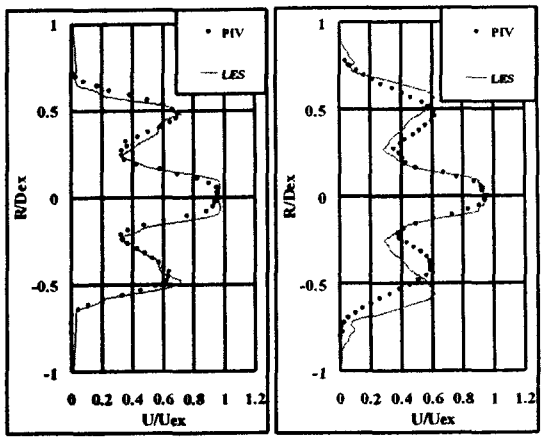

(a) X=1.0Dex (b) X=1.5Dex

Fig. 12 Comparisons of time-averaged radial profiles of axial velocity component between PIV data and LES results

Influence of inflow turbulence on the mixing

It is well known that the mixing characteristics of a jet flow are strongly affected by inflow turbulence in the nozzle. In order to clarify the role of inflow turbulence, we conducted the LES calculation in which inflow turbulence in the mixer nozzle was neglected and compared with the measurement and previous calculation with inflow turbulence.

Figure 13 shows the contours of the calculated velocity magnitude in the case when the inflow turbulence was neglected. It is observed that the high velocity core regions from upper and lower lobes extended further downstream compared with the former calculation result in which the inflow turbulence was imposed.

The radial profiles of the axial velocities on the A-A plane were compared in Fig. 14. A distinctive feature is appeared in the core regions downstream of upper and lower lobes, where the calculation result without inflow turbulence shows higher peak velocity at 1.0Dex and lower peak velocity at 1.5Dex. This suggests that the inflow turbulence enhances a mixing of core flows from lobes to some extent of downstream, but produces less mixing at further downstream.

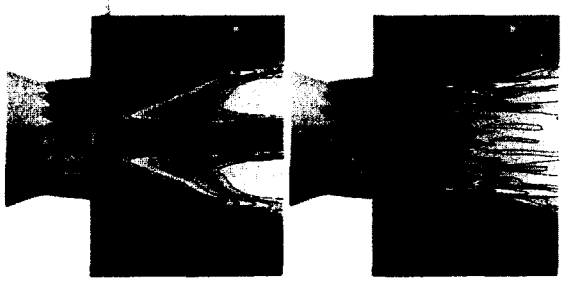

(a) A-A plane (b) B-B plane

Fig. 13 Time-averaged calculated velocity contours without turbulent inflow at mixer nozzle inlet

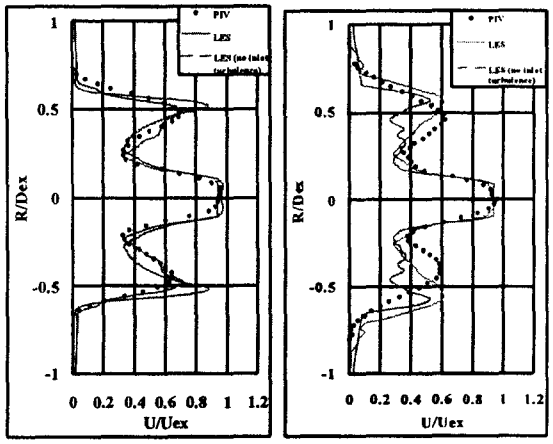

(a) X=1.0Dex (b) X=1.5Dex

Fig. 14 Comparison of time-averaged radial profiles of axial velocity component between results with and without turbulent inflow

Conclusions

1. The flowfield downstream of CD nozzle was simulated using both of large eddy simulation and RANS using L-B model. LES predicted more reasonable flow structure.
2. LES calculation of a 18-lobe convoluted mixer nozzle was conducted and compared with the measured data acquired using PIV method. LES calculation is capable of predicting the mixing characteristics of a complicated mixer nozzle.

Acknowledgment

This study was conducted under the entrustment contract with the New Energy and Industrial Technology Development Organization (NEDO) as a part of the National Research and Development Program (Industrial Science and Technology Frontier Program) of Ministry of Economy Trade and Industry (METI).

The authors would like to acknowledge the contribution of Mr. Isawa of IHI for the PIV measurement.

References

1) Nakamura,Y and Oishi,T, "Research and Development of Mixer-Ejector Nozzle", Proceedings of the International Gas Turbines Congress 1999 Kobe, 1999, p219-224.
2) Baldwin, B.S. and Lomax, H., "Thin-Layer Approximation and Algebraic Model for Separated Turbulent Flows", AIAA 78-257. 1978.
3) Lam, C.K.G. and Bremhorst, K.A., "Modified Form k- ε model for Predicting Wall Turbulence", ASME, J. of Fluids Engineering, Vol. 103, 1981, pp456-460.
4) Freund, J.B., 'Direct Simulation of A Mach 1.92 Jet And Its Sound Field', AIAA/CEAS 98-2291, 1998.
5) Choi, D. et al. "Large Eddy Simulations of High-Reynolds Number Jet Flows", AIAA 99-0230, 1999.
6) Yamamoto, K., et al, 'Experimental Investigation of Shock-Cell Noise Reduction for Single Stream Nozzles in Simulated Flight', NASA CR 3845, 1984.
7) Ooba, Y., et al, 'Large Eddy Simulation Analysis of Lobed Mixer Nozzle', Proceedings of 1st International Conference on Computational Fluid Dynamics, pp159-160, 2000.
8) Ooba, Y., et al, 'Large Eddy Simulation Analysis of a 18-Lobe Convoluted Mixer Nozzle', AIAA2002-0717, 2002.
9) Smagorinsky, J., "General circulation experiments with the primitive equations, I The basic experiment", Monthly Weather Review, 91, pp99-164, 1963.